

RECORDING TIME DELAY OF SUDDEN MAGNETIC STORM AT DIFFERENT MAGNETIC OBSERVATORIES: ANALYSIS OF INDIVIDUAL EVENTS

© 2025 Yu. S. Zagainova^{a, *}, S. V. Gromov^a, L. I. Gromova^a, and V. G. Fainshtein^b

^a*Pushkov Institute of Terrestrial Magnetism, Ionosphere, and Radio Wave Propagation, Russian Academy of Sciences (IZMIRAN), Moscow, Troitsk, Russia*

^b*Institute of Solar–Terrestrial Physics, Siberian Branch, Russian Academy of Sciences (ISTP SB RAS), Irkutsk, Russia*

*e-mail: yuliazaganova@mail.ru, yuliazag@izmiran.ru

Received March 03, 2025

Revised May 03, 2025

Accepted May 22, 2025

Abstract. The problem of simultaneous detection of a sudden commencement (SC) and a main pulse (MI) of geomagnetic storm by different magnetic stations are discussed using the example of two SC-events of March 17, 2013 and March 17, 2015. Interplanetary coronal mass ejections and associated shock waves that caused the studied the SC-events are identified with coronal mass ejections observed near the Sun, the source regions of which were in different solar hemispheres. The linear projected velocities of the two sampled coronal mass ejections are very different, which provided a marked difference in the velocities of the associated interplanetary shock waves. Trends were found in the form of a linear or quadratic relationship for each SC-event analyzed, using second time resolution data, the latitude and longitude of the magnetic station on the Earth's surface were associated with detection start times of SC and MI. We used an authorial approach to detection start times of SC and MI. It is concluded that detection start times of SC and MI can differ from a few seconds to more than one minute on magnetic observatories located at different geographical latitudes and longitudes. The magnetic stations that first detection of SC and MI in each analyzed SC-event were identified. It has been suggested that the position of station the first to detect SC and MI depends on the characteristics of the interplanetary shock waves affecting the Earth's magnetosphere.

Keywords: *coronal mass ejection, solar wind, magnetosphere, interplanetary shock wave, sudden commencement of geomagnetic storm*

DOI: 10.31857/S00167940250514e3

1. INTRODUCTION

The impact of an interplanetary shock wave (ISW) on the Earth's magnetosphere often leads to a short-term but significant in intensity perturbation of the geomagnetic field, which is then accompanied by a geomagnetic storm. Such a perturbation of the Earth's magnetic field is called the sudden onset of a geomagnetic storm and is denoted by the abbreviation SC (*Sudden Commencement* [Curto et al., 2007] or the old designation SSC (*Storm Sudden Commencement*) is used.) Many papers have been devoted to the study of SC (see, for example, the monographs [Akasofu and Chapman, 1975; Nishida, 1980] as well as a number of papers published in recent years [Smith et al., 2021; Singh et al., 2024; Zhou and Lüher, 2022; Veretenenko et al., 2020; Bocchialini et al., 2018; Fathy et al., 2018; Araki and Shinbori, 2016] and the literature cited therein). SC is recorded almost simultaneously over the entire Earth as a sharp increase in the horizontal *H component* of the Earth's magnetic field, including at magnetic stations and observatories located at different locations on the Earth's surface. SC is also registered on spacecraft (SC) equipped with highly sensitive magnetometers, e.g., on GOES, THEMIS series satellites (e.g., [Pezzopane et al., 2019]).

It is considered that SC often appears at high-latitudinal stations earlier than at low-latitudinal stations. It was established that the sudden change in time of the *H-component* of the geomagnetic field during the SC-event has a global character. The response to the impact of the ICE on the magnetosphere is manifested to a greater or lesser extent in the entire magnetosphere. In [Araki, 1994], a physical model that can explain the global structure of geomagnetic sudden onset was proposed. There are various lists of reported SCs. For example, in [Mayaud, 1975], a list of SCs for 100 years was formed and studied. The *International Service of Rapid Magnetic Variations* (SRMV) compiled the most accurate lists of SC-events [Curto et al., 2007].

The problem of the simultaneity of SCs registered by different magnetic stations, which reflects the character of the interaction between the interplanetary shock wave (ISW) and the magnetosphere, special in each particular case, is considered separately in solar-terrestrial physics. There are very few works devoted to this problem, which is explained by the inaccuracy of SC registration, especially at low latitudes. The results of early studies of the SC simultaneity problem are presented, for example, in the monograph [Akasofu and Chapman, 1975], where the following conclusions were postulated based on the results of a number of works: (i) differences in the time of SC registration are a few seconds; (ii) the hemisphere where SC is registered first is controlled by the Sun; (iii) SC is registered a few minutes earlier at high latitudes than at low latitudes (for details and references to relevant works, see [Akasofu and Chapman, 1975]). The accuracy of SC registration by modern instruments and the accuracy of the reference to universal time UT allow us to revise the old results.

In most cases, the sudden change in time of the *H-component* of the geomagnetic field is studied using data with a minute time resolution, including 1-minute data to determine the moment of the beginning of SC registration. However, nowadays many magnetic stations and observatories are equipped with highly sensitive magnetometers with a second and even higher temporal resolution. Magnetic data with higher temporal resolution than 1 min allow us to study the fine structure of SC. The most striking feature of the fine structure of the SC is a sharp short-term increase by several times of the values of the *H-component* of the geomagnetic field, which is called the main *impulse* and denoted MI (*Main Impulse*). The main impulse can be preceded by a preliminary impulse PI (*Preliminary Impulse*)— a weaker perturbation of the geomagnetic field of the opposite sign. Some researchers include in the fine structure of SC still oscillations of magnetic field characteristics in the frequency range up to several Hertz, which can precede PI and MI [Parkhomov, 1985; Parkhomov et al., 2017]. MI is believed to be produced by large-scale electric currents in the ionosphere [Nishimura et al., 2016]. The system of electric currents determining MI has been analyzed in numerical calculations (see [Sun et al., 2015] and the literature cited there). The physical mechanisms of PI generation have not been fully established, although different variants of them were considered in publications [Araki, 1977; Kikuchi and Araki, 1979].

In our recent work [Zagainova et al., 2024], we analyzed magnetic data with a second time resolution on the example of two SC events from June 22, 2015 and July 16, 2017. It was shown that due to the impact of the MUV on the magnetosphere, the registration of such fine structure elements as the moment of the onset of SC and MI registration by ground-based magnetic stations located at different geographic latitudes and longitudes does not occur simultaneously. The time of SC and MI registration at different stations differs from several seconds to more than one minute. The first magnetic stations that registered SC and MI were noted. In addition, on the plots of the appearance of SC and MI as functions of the latitude of magnetic stations ϕ and universal time UT, trends were found according to which, on average, the greater the latitude of the station at which SC and MI are registered, the later these perturbations of the geomagnetic field are observed there. We assumed that the deviations of our results from the published results of the past years (for example, in the monograph [Akasofu & Chapman, 1975]) are related to the maximum velocity of the CME near the Sun. Thus, the maximum linear projected velocity of the CME of June 21, 2015, associated with the SC event of June 22, 2015, was $V_{lin} = 1366$ km/s, and for the CME of June 14, 2017, associated with the SC event of June 16, 2017. — $V_{lin} = 1200$ km/s.

In the present work, we decided to continue the study of SC properties using data with a second time resolution on the example of two more SC events. We selected two SC events from March 17, 2013, and March 17, 2015, caused by interplanetary shock waves associated with CMEs with lower velocity values near the Sun. Thus, the maximum line-projected velocity of the CME of

March 15, 2013 associated with the SC event of March 17, 2013. – $V_{lin} = 1063$ km/s, and for the CME from March 15, 2015, associated with the SC event of March 17, 2015, was $V_{lin} = 799$ km/s. As in our previous work, we considered the issue of the simultaneity of SC and MI registration by magnetic stations located at different locations on the Earth's surface, found out the presence of the above-mentioned trends, and carried out a preliminary analysis of the influence of the characteristics of the CME that affected the magnetosphere on some features of SC and MI registration by different magnetic stations.

The purpose of our work is to study the issue of simultaneous registration of SC and MI by magnetic stations located in different places on the Earth's surface, including the study of the nature of the appearance of SC and MI as functions of the latitude of magnetic stations ϕ and world time UT, as well as a preliminary analysis of the influence of the characteristics of the MCE that affected the magnetosphere on some features of SC and MI registration by different magnetic stations.

2. DATA AND METHODS OF ANALYSIS

2.1 Selection and description of SC events and their sources

Two SC events from the SC catalog presented by the IAGA (*International Association of Geomagnetism and Aeronomy*) international geomagnetic index service, dated March 17, 2013 at 05:59 UT and March 17, 2015 at 04:45 UT, were selected for analysis. These events are characterized by the following properties. First of all, it was confirmed that the SC indeed reflects the impact of MUVs on the magnetosphere. Information about the existence of such ICEs was obtained from data from the CfA Interplanetary Shock Database - Wind website (https://lweb.cfa.harvard.edu/shocks/wi_data/) and, additionally, from OMNIWeb Service data (<https://omniweb.gsfc.nasa.gov>) with minute resolution, where the ICE stands out as a sharp spike in the main magnetohydrodynamic parameters of the solar wind: density, temperature, plasma velocity, and magnetic field [Hundhausen, 1972].

According to the "List of Richardson/Cane ICMEs" catalog (<https://izw1.caltech.edu/ACE/ASC/DATA/level3/icmetable2.htm>) and the characteristics of the solar wind after the SC according to OMNIWeb Service data, the MUVs that caused the SC were followed by interplanetary CMEs (ICMEs). These ICMEs were identified with halo ICMEs recorded near the Sun by the LASCO C2 and C3 coronagraphs [Brueckner et al., 1995] on board the SOHO spacecraft [Domingo et al., 1995].

The SC-event of March 17, 2013 corresponds to the CME first registered by the LASCO C2 coronagraph on March 15, 2013 at 07:12 UT, and the SC-event of March 17, 2015 corresponds to the CME first registered on March 15, 2015 at 01:48 UT. These CMEs occurred in different hemispheres of the Sun (northern and southern) and had different modulo latitudes and different

longitudes. We will consider the location of the CMEs to coincide with the location of the associated solar flare. According to the halo CME catalog (https://cdaw.gsfc.nasa.gov/CME_list/halo/halo.html), the place of origin of the first CME is characterized by coordinates N11E12, the second CME– by coordinates S22W25, i.e., the first CME originated in the Northern Hemisphere of the Sun, the second CME - in the Southern Hemisphere. The linear projected velocities for the two CMEs were 1063 and 719 km/s, respectively.

The data of the Harvard-Smithsonian Center for Astrophysics (https://www.cfa.harvard.edu/shocks/wi_data) were used to determine the characteristics of the ICE. These data allowed us to determine the velocity of the ICE, the orientation of the normal to the ICE front in three-dimensional space, and other characteristics of the ICE. On this site, the parameters of the ICE are found by eight different methods and the values of these parameters averaged over the values found by different methods are given. In the following, we will use these average values of the ICE parameters. Thus, for the SC event of March 17, 2013, the MUV velocity $\langle V_{sh} \rangle = 740.3$ km/s, the plasma density jump (compression) is $\langle 2.87 \rangle$, the latitude normal $\langle \theta \rangle = 6.007$ deg, and the longitude normal $\langle \varphi \rangle = 178.173$ deg in the geocentric solar-ecliptic coordinate system (GSE). In this case, the orientation of the normal to the MUV front almost coincides with the Sun– Earth direction. For the March 17, 2015 event $\langle V_{sh} \rangle = 494$ km/s, the plasma density jump is 2.45, latitude normal $\langle \theta \rangle = 25.796$ deg, longitude normal $\langle \varphi \rangle = 204.172$ deg. For each selected SC event, we used 1-second time-resolved data from different INTERMAGNET network magnetic observatories (<https://www.intermagnet.org>), which provide magnetic data from highly sensitive magnetometers with both minute and second time resolution. In total, data from 70 stations located on the Earth's surface at different geographic latitudes and longitudes were used: AAE, ABK, AMS, API, ASP, BDV, BEL, BLC, BOU, BOX, BRD, BRW, BSL, CDD, CKI, CLF, CMO, CNB, CSY, CTA, CYG, CZT, DED, DLT, DRV, EBR, EYR, FCC, FRD, FRN, GNG, GUA, HBK, HER, HLP, HON, HRN, IPM, IQA, KAK, KDU, KNY, KOU, LRM, LYC, LZH, MAW, MBO, MCQ, MEA, MMB, NEW, NUR, OTT, PAF, PEG, PHU, PPT, RES, SBA, SHU, SIT, SJG, STJ, TAM, TUC, UPS, VIV, WIC, YKC.

For time referencing of data from all magnetic stations, UT world time is used. To determine the position of a magnetic station on the Earth's surface, we used the geographic latitude φ and longitude λ of the stations, which was converted from geographic longitude to longitude relative to the "noon longitude", where $\lambda = 0^\circ$, i.e., geographic longitude on the Sunlit hemisphere of the Earth, where noon was observed at the time of the beginning of SC. We were interested in how far away each station was from the "noon longitude". Using the values of the geographic longitude of each

station and the SC start time in UT, we determined the longitude λ of the magnetic station positions relative to the "noon longitude" where noon was observed at the time of the arrival of the ICVM to Earth at 12:00 LT local time. The longitude of λ stations was calculated as the minimum difference between the geographic longitude of the station and the geographic longitude at the "noon line". Thus, if the station was located on the "noon longitude line" at the time of SC onset, then $\lambda = 0^\circ$. If the station was observed east of the "noon longitude", then λ takes the values $(-180^\circ; 0^\circ)$, with the values $\lambda = (-180^\circ; -90^\circ)$ corresponding to the station's position on the non-sunlit hemisphere of the Earth. Correspondingly, if a magnetic station at the time of SC onset is located west of the "noon longitude", then $\lambda = (0^\circ; 180^\circ)$, and the values $\lambda = (90^\circ; 180^\circ)$ should be attributed to stations located on the night side of the Earth. Negative values of latitude ϕ are assigned to the data of observations of stations of the Southern Hemisphere of the Earth, and positive values— of the Northern Hemisphere of the Earth. The values of geographic latitude and longitude of magnetic stations are available in the INTERMAGNET network.

For each considered SC event from the magnetic station observations of the *H-component* of the geomagnetic field with 1-minute and 1-second time resolution, the time range within ± 5 min from the moment of SC registration determined from the 1-minute data was selected. Recall that for the event of March 17, 2013, the time at 05:59 UT was taken as the SC onset time, and for the event of March 17, 2015. - 04:45 UT. The studied SC events are associated with strong geomagnetic storms. Thus, the magnetic storm of March 17, 2013 with a sudden onset of G3 class, $Dst_{\min} = -132$ nTL, is noted as the most powerful storm in 2013. The March 17, 2015 magnetic storm with sudden onset was the most powerful storm in 2015 and is categorized as class G4, $Dst_{\min} = -234$ nTL.

Fig. 1.

As an example, Fig. 1 (*a, b*) shows the magnetic field variations at the Honolulu Low Latitude Magnetic Observatory (HON, USA, Hawaii) for selected SC events. In the plots of Fig. 1, the second data (dashed line) are scaled to the scale of the minute data (solid line). It can be seen that they do not coincide: the main difference is that the *H-component* of the magnetic field increases more steeply for the data with a second time resolution.

In addition, Fig. 1(*c, e*) shows the magnetic field variations on the example of the midlatitude obs. Chambon-de-Foret (CLF, France) and low-latitude magnetic obs. Tamanrasset (TAM; Algeria) for the SC event of March 17, 2013. On the right side of Fig. 1(*d, e*), we present the variations of the *H* field *component* at the low-latitude stations Dalat, USA (DLT) and Learmonth, Australia (LRM) for the SC *event* of March 17, 2015. Just as in Fig. 1(*a, b*), the plots in Fig. 1(*c– e*) combine data with minute and second time resolution. The same processing was performed for each magnetic observatory where second time-resolved data are available for the selected SC events. The

following paper presents the results of analyzing only the 1-second observational data for each magnetic observatory.

2.2 SC fine structure and methods for analyzing it

We used a certain approach to find the onset of SC and MI, which is detailed in our paper [Zagainova et al., 2024]. Here, we only note additionally that before determining the moments of the onset of SC and MI registration by magnetic stations, we performed in some cases a preliminary normalization of the horizontal component of the geomagnetic field $H(t)$, including subtraction of the background component and normalization by 1.0 at the time interval ± 2 min from the official onset of SC registration using 1-min data. We denote the resulting normalized function by $H_n(t)$.

Fig. 2.

Fig. 2a shows the $H_n(t)$ dependences for the SC event of March 17, 2013 on the example of a number of stations: API, ASP, BSL, CTA, DLT, FRD, GUA, HON, IPM, KDU, KOU, MAW, MBO, UPS. Fig. 2b shows similar $H_n(t)$ dependencies, but for the SC event of March 17, 2015, using the example of stations: ASP, BDV, CTA, CYG, EBR, GNG, HON, IPM, KAK, KDU, KOU, LRM, MBO, PPT, SJG, TAM. We note that the increase of the H- component of the field is not instantaneous. It can be visually determined that for different stations the moment of the beginning of the rapid increase in the values of the H component of the magnetic field occurs at different times. In addition, the moment of rapid increase in the field values is preceded by a time interval with a smoother increase in the values of the H-component of the field, where H_n varies from $\sim 5\%$ to $\sim 20\%$. We define the time moment corresponding to the rapid increase of the field as the main impulse MI, and we refer the time moment corresponding to the beginning of the smooth increase of the H -component of the field to the moment of the beginning of SC registration.

Recall from [Zagainova et al., 2024] that the determination of the moments of the beginning of SC and MI registration was performed visually and/or from the analysis of the curve of the numerical time derivative from $H_n(t)$ or from $H(t)$. The MI registration onset time t_{MI} was first determined as the moment of the beginning of a sudden change in the behavior pattern (rise or minimum) of the time derivative. The moment of the time of the beginning of registration of the sudden onset t_{SC} of the magnetic observatory was defined as the beginning of slow growth of the values of the horizontal H -component of the Earth's magnetic field. For some stations, where for ~ 2 min from the moment of MI onset there are no clearly pronounced extrema and/or pronounced areas of rise/decline of the horizontal component of the geomagnetic field values and the H -component of the field clearly assumes a minimum value, SC was found visually as the moment of the beginning of the growth of the H -component of the field values. Often for the data of a number of magnetic stations, small extrema of the H -component of the field were located between the beginning of SC

and MI registration (Fig. 2). In such cases, the beginning of SC registration was determined by the minimum of the numerical time derivative of $H_n(t)$ or $H(t)$ at the time interval ~ 2 min from the time of the beginning of MI registration. When t_{SC} could not be unambiguously identified visually or by analyzing the numerical time derivative of $H_n(t)$ or $H(t)$, we approximated $H_n(t)$ on small time scales $\sim \pm(1-2)$ min from the onset of MI by analytical exponential functions of the form $y_m(t) = y_0 + A \exp((t-t_0)/\tau)$. The parameters of the approximating function were chosen to provide the best agreement between the time-dependent behavior of this function and the measured dependence $H_n(t)$. In addition to such fine structure elements as SC and MI, the data from some stations additionally distinguish a preliminary PRI (*Preliminary Recovery Impulse*) or PI, which is also preceded by a short interval of smooth field increase; we also determine its onset for such stations as SC (the methodology for determining the time of the onset of SC and MI registration is described in more detail in [Zagainova et al., 2024]).

3. RESULTS

Fig. 3 shows the variations with time of the interplanetary magnetic field (IMF) and solar wind parameters, as well as geomagnetic activity on Earth, expressed by the *SYM-H* storm index (the one-minute analog of the *Dst* index), on March 17, 2015. The arrows indicate the SC registration times caused by the arrival of the interplanetary shock wave associated with the CMB of March 15, 2015, and the leading edge of the magnetic cloud (MC). The registration times of the MUV and the region of shock-compressed plasma behind the shock front (SHEATH), as well as the leading edge of the MC, are indicated according to the classification of events in the solar wind [Ermolaev et al., 2009] presented in the catalog on the website (<http://www.iki.rssi.ru/omni/catalog/>). The MUV and MC registration moments are determined according to the List of Richardson/Cane ICMEs catalog (<https://izw1.caltech.edu/ACE/ASC/DATA/level3/icmetable2.htm>).

Fig. 3.

The March 17, 2015 magnetic storm was more intense (*SYM-H* ~ -200 nTL) of those considered in this paper, but the SC was recorded at a lower velocity ($V \sim 500$ km/s) but denser solar wind flow than for the March 17, 2013 event. The density jump was from 15 to 30 cm^{-3} . The dynamical pressure increased sharply from ~ 8 to almost 25 nPa, and the *Bz* component of the MMP was positive.

Fig. 4a, b show the plots of the appearance of SC and MI, respectively, as a function of latitude ϕ and world time UT for the March 17, 2015 event, and Fig. 4 (in- d) - plots of the appearance of SC and MI as a function of longitude λ and world time UT. It is noteworthy that all

plots linking the moments of SC and MI appearance and the latitude/longitude of the magnetic station have trends in the form of linear or quadratic dependence.

Fig. 4.

Plots of SC occurrence as a function of station latitude φ and world time UT show these trends as regression lines: in the Northern Hemisphere $f_{\varphi N}(t) = 6.93891 + 2.77336t - 0.03971t^2$ (correlation coefficient $r = 0.41$) and in the Southern Hemisphere of the Earth $f_{\varphi S}(t) = -38.08892 - 0.20828t$ ($r = 0.24$) (Fig. 4a). Plots of SC occurrence as a function of the difference between the geographic longitude of the station and the "noon line", where $\lambda = 0$, and the universal time UT from the onset of SC recording show quadratic trends $f_{\lambda W}(t) = -0.02961t^2 + 4.72296t - 5.66109$ ($r = 0.72$) for stations at longitudes west of the "noon line" and $f_{\lambda E}(t) = 0.07256t^2 - 5.89565t - 4.46954$ ($r = 0.46$) for stations located at the time of SC onset at longitudes east of the "noon line" (Figure 4c). Figure 4c shows that the DLT and LRM magnetic observatories, which first registered SC at 04:44:24 UT, were located near the "noon line", i.e., on the Sunlit hemisphere of the Earth at the time of the SC onset.

The total number of stations whose second-resolution data were used for the analysis— $N=58$. The difference Δt_{SC} between the first and the last of the 58 stations was 58 s, and $\Delta t_{MI} = 136$ s, i.e., the difference ($t_{MI} - t_{SC}$) is not constant and varies from station to station.

Similar dependences for MI also showed trends both for the stations of the Northern Hemisphere of the Earth and for the stations of the Southern Hemisphere (Fig. 4b, d). Thus, plots of the onset of MI registration as a function of station latitude φ and world time UT show a quadratic trend in the Northern Hemisphere $f_{\varphi N}(t) = -0.0031t^2 + 0.82215t + 5.50248$ ($r = 0.58$) and a weak linear trend in the Southern Hemisphere $f_{\varphi S}(t) = -0.19931t - 35.55957$ ($r = 0.5$). The plots of MI registration as a function of the difference between the geographic longitude of the station and the "noon line" λ and time t can also show trends (Fig. 4g). Thus, for stations located at the onset of the SC event at longitudes east of the "noon line"— $f_{\lambda E}(t) = -0.35549t - 75.73539$ ($r = 0.43$), west of— $f_{\lambda W}(t) = -0.01373t^2 + 2.51838t + 10.32088$ ($r = 0.4$). The first station to register MI at 04:44:47 UT was the Southern Hemisphere Earth station GNG, which at the time of the start of SC was on the Sunlit side of the Earth in the longitude sector $\Delta \lambda$ from 0° to 90° .

Shown below are Fig. 5 and Fig. 6 for the SC event on March 17, 2013, arranged similarly to Figures 3 and 4 for the event on March 17, 2015. Figure 5 shows the MMP and solar wind parameters and geomagnetic activity expressed by *SYM-H* on March 17, 2013. As in Fig. 3, the arrows indicate the moments of SC registration (caused by the arrival of the MUV associated with the CME of March 15, 2015) and the leading edge of MC. The moments of MUV and MC

registration were determined from *the* data of the catalog "*List of Richardson/Cane ICMEs*" (and are indicated according to the classification of solar wind events [Ermolaev et al., 2009]).

Fig. 5.

Fig. 6.

The sudden onset of the SC storm is reflected by a sharp jump in the *SYM-H* index (*SYM-H* panel in Fig. 5). In this case, on March 17, 2013, we observed a high-speed solar wind flow with a velocity $V \sim 700$ km/s with a density jump from 3 to 10 cm⁻³, the dynamic pressure increased sharply from 4 to 12 nPa and further increased to 20 nPa, the *Bz* component of the MMP was weakly negative, after SC it changed sharply to -15 nTL, and the magnetic storm reached *SYM-H* ~ -130 nTL. Note that in both considered cases on March 17, 2013 and March 17, 2015, the dynamic pressure pulse associated with the MLE was mainly due to a relatively strong density increase at its front.

The total number of magnetic observatories and stations for this event is $N = 52$. The first station that registered SC at 05:59:06 UT is TAM, $\Delta t_{SC} = 73$ s, and the first station that registered MI at 05:59:48 UT is Dumont d'Urville (DRV, Antarctica), station latitude $\varphi = -67^\circ$, $\Delta t_{MI} = 172$ s.

Fig. 6 shows the plots of the moments of SC and MI occurrence as functions of geographic coordinates and world time UT for the event from March 17, 2013. The plots of the SC onset moment as a function of station latitude φ and world time UT show linear trends in the Northern Hemisphere $f_{\varphi N}(t) = 0.35227t + 31.569$ (correlation coefficient $r = 0.3$) and in the Southern Hemisphere of the Earth $f_{\varphi S}(t) = -0.14335t - 35.34004$ ($r = 0.32$) (Fig. 6a). The plot of SC occurrence as a function of the difference between the station's geographic longitude and the "noon line" λ and world time UT shows a weak linear trend $f_{\lambda W}(t) = 1.18067t + 58.05326$ ($r = 0.3$) for stations at longitudes west of the noon line" and a weak quadratic trend $f_{\lambda E}(t) = 0.125t^2 - 5.37261t - 63.03734$ ($r = 0.2$) for stations located at the time of SC onset at longitudes east of the "noon line" (Fig. 6c). Figure 6c shows that the mid-latitude TAM station at the time of the beginning of SC registration was located in the longitude sector $\Delta \lambda$ from 0° to -90° , i.e., in the eastern part of the Sunlit hemisphere of the Earth.

Similar dependences for MI also showed trends both for the stations of the Northern Hemisphere of the Earth and for the stations of the Southern Hemisphere (Fig. 6b). Thus, the plots of MI onset as a function of station geographic latitude φ and world time UT show a quadratic trend in the Northern Hemisphere $f_{\varphi N}(t) = -0.00145t^2 + 0.60607t - 12.10813$ ($r = 0.4$) and a very weak trend in the Southern Hemisphere of the Earth $f_{\varphi S}(t) = 0.004t - 39.46283$ ($r = 0.02$). In the plots of the onset MI registration as a function of station longitude and world time UT, quadratic trends can be identified (Fig. 6g). Thus, for stations located at the onset of the SC event at longitudes east of

the "noon line" – $f_{\lambda E}(t) = -0.01093t^2 + 2.54807t + 4.20849$ ($r = 0.64$), west of – $f_{\lambda W}(t) = 0.04062t^2 - 4.31653t + 16.71948$ ($r = 0.5$). The first station to record MI was the Southern Hemisphere Earth station DRV, which at the time of the SC onset was located on the Sunlit side of the Earth in the longitude sector $\Delta \lambda$ from 0° to 90° .

The reason for the detected regularities in the plots of SC and MI registration moments at magnetic observatories as functions of their geographic coordinates and universal time UT, apparently, lies in the not yet known peculiarities of the propagation of perturbations in the magnetosphere that arose after the impact of the interplanetary shock wave on it. We can assume that, based on the dependences $f_{\phi N}(t)$, $f_{\phi S}(t)$, $f_{\lambda E}(t)$ and $f_{\lambda W}(t)$ obtained by us, it will be possible to obtain more precise information about the physical mechanisms of SC and MI generation.

The results obtained in this work, as well as the results presented in our previous work [Zagainova et al., 2024], indicate that earlier SC is registered at stations located not at all at high-latitude (subpolar and polar) stations, as claimed in earlier works (see, for example, the monograph [Akasofu & Chapman, 1975]). As shown above, in the SC event of March 17, 2013, the first to record the sudden onset of the storm was the TAM station at latitude $\phi = 23^\circ$, in the SC event of March 17, 2015, – stations DLT at latitude $\phi = 11.9^\circ$ and LRM at latitude $\phi = -21^\circ$, in the SC event of June 22, 2015, – KOU station at latitude $\phi = 5^\circ$, in the SC event of July 16, 2017, – AMS station at latitude $\phi = -38^\circ$.

We hypothesized earlier that the latitude of the station that first recorded the SC depends on the velocity of the interplanetary CME and the associated MUV, i.e., the higher the velocity of the CME associated with the SC event, the more low-latitude magnetic stations respond earlier to the arrival of the MUV. As a result of the studies, everything turned out to be not so unambiguous. Thus, the speed of the CME according to the WIND spacecraft data for the March 17, 2013 event is about 740 km/s, and for the March 17, 2015 event is about 477 km/s, i.e., in the first case is greater than in the second. Interestingly, the magnitude of the MUV velocity correlates with the linear projected velocity of the CME in the field of view of the LASCO C2 and C3 coronagraphs – 1063 and 719 km/s, respectively. However, for the SC event of March 17, 2015, magnetic observatories located closer to the equator were the first to respond as a result of the interaction between the CMB and the Earth's magnetosphere than in the case of the SC event of March 17, 2013. For this reason, we additionally assumed that the results obtained may also depend on the orientation of the ECC front.

For the SC events studied in this work and the SC event of June 22, 2013 analyzed in [Zagainova et al., 2024], the characteristics of the ICE are known according to the Harvard-Smithsonian Center for Astrophysics. It turned out that the MUV velocity $\langle V_{sh} \rangle$ for the case of the

SC event of June 22, 2015 exceeds the MUV velocities for the SC events investigated in this paper and was $\langle V_{sh} \rangle = 776$ km/s. In addition, the orientation of the normal to the ICE front for the SC events of March 17, 2013 and June 22, 2013 almost coincides with the direction "Sun– Earth". Recall that for the SC event of March 17, 2013, latitude normal $\langle \theta \rangle = 6.007^\circ$, and longitude normal $\langle \varphi \rangle = 178.173^\circ$ at GSE, and for the SC- event of June 22, 2013, latitude normal $\langle \theta \rangle = -4.901^\circ$, longitude normal $\langle \varphi \rangle = 186.201^\circ$. Figure 7 illustrates the orientation of the MUV in two mutually perpendicular planes XZ (perpendicular to the ecliptic plane - panels *a, c, e*), and XY (in the ecliptic plane; panels *b, d, f*) in the GSE coordinate system. For the SC event of March 17, 2013, the first to respond was the magnetic station TAM on the Sunlit side of the Earth at latitude $\varphi = 23^\circ$, and for the SC event of June 22, 2013,– station KOU, also located at the time of the onset of the magnetic storm on the Sun-controlled side of the Earth, at latitude $\varphi = 5^\circ$. It turns out that for these two SC events, the assumption that the higher the speed of the MST, the more low-latitude stations will react first to the arrival of the MST to the Earth is fulfilled.

The SC-event of March 17, 2015 was characterized by a much lower ICE velocity $V_{sh} = 494$ km/s than for the other SC-events considered by us. However, in addition to the relatively low ICE velocity, this SC event was distinguished from the others by the fact that the angle between the normal to the ICE front and the direction "Sun– Earth" was much higher. Thus, latitude normal $\langle \theta \rangle = 25.796^\circ$, longitude normal $\langle \varphi \rangle = 204.172^\circ$. If we conditionally look at the Earth from the side of the Sun, then the ICE approached the Earth as if from the side from the right and from the bottom (from the southern hemisphere of the heliosphere), i.e. the considered case can be represented as a "non-lobal" interaction" MUV and the Earth's magnetosphere.

Taking into account the results obtained in this paper and in [Zagainova et al., 2024], we have considered four SC events for the simultaneity of SC registration by different magnetic stations, which allowed us to draw some conclusions (see the "Conclusion" section) and assumptions as a preface for further work. In particular, we believe that in the future it is necessary to consider separately on sufficient statistical material SC-events caused by MUVs with the orientation of the normal to the front almost coinciding with the direction "Sun– Earth".

4. CONCLUSION

The analysis of the SC and MI occurrence plots as a function of the geographic coordinates of magnetic observatories and UT world time using data with a second time resolution for two SC events of March 17, 2013 and March 17, 2015, taking into account the results from [Zagainova et al., 2024] allowed us to draw the following conclusions.

- The sudden onset of the SC geomagnetic storm according to the data with second resolution is registered by geomagnetic observatories located at different geographic latitudes and longitudes at different times.
 - For all the considered events, there are trends in the plots of the occurrence of SC and MI as a function of geographic coordinates of the magnetic observatories and universal time UT in the form of linear or quadratic dependence.
 - In the considered events, the magnetic observatories located on the Sunlit side of the Earth are the first to register SC.
 - Based on the results for the two SC events of March 17, 2013 and June 22, 2015, the following condition is met: when the normal to the interplanetary shock wave is almost parallel to the Sun–Earth direction, the magnetic station that first registered SC is located at lower latitudes if the velocity of the MUV is greater.
- From the analysis of three SC events from March 17, 2013, June 22, 2013, and March 17, 2015, it appears that for an SC event with a relatively small MUV velocity and a large angle of deviation of the normal to the interplanetary UW relative to the Sun–Earth direction, two stations at low latitudes were the first to simultaneously record an SC event, which is more similar to the situation with a UW with a large velocity and a small angle of deviation of the normal to the interplanetary UW relative to the Sun–Earth direction.

FUNDING

This work was financially supported by the Ministry of Science and Higher Education of the Russian Federation.

ACKNOWLEDGEMENTS

The authors of this paper thank the LASCO/SOHO team for the opportunity to freely use the data from this tool. We also thank the creators of the catalogs The full SOHO/LASCO CME CATALOG (https://cdaw.gsfc.nasa.gov/CME_list/index.html), SOHO/LASCO HALO CME CATALOG (https://cdaw.gsfc.nasa.gov/CME_list/halo/halo.html), OMNIWeb Service (<https://omniweb.gsfc.nasa.gov>), Near-Earth Interplanetary Coronal Mass Ejections Since January 1996 (<https://izw1.caltech.edu/ACE/ASC/DATA/level3/icmetable2.htm>), Harvard-Smithsonian Center for Astrophysics with data on the orientation of the normal to the MCE front with respect to the line "Sun–Earth" CfA Interplanetary Shock Database - Wind (www.cfa.harvard.edu/shocks/wi_data), INTERMAGNET (<https://www.intermagnet.org>) and the

catalog with classification of events in the solar wind (<ftp://ftp.iki.rssi.ru/pub/omni/catalog>) [Ermolaev et al, 2009] for the possibility of free use of the data given in them.

REFERENCES

1. *Akasofu S.I., Chapman S.* Solar-terrestrial physics. 2nd. Translated from English. Moscow: Publishing house "Mir", 512 p. 1975.
2. *Ermolaev Yu.I., Nikolaeva N.S., Lodkina I.G., Ermolaev M.Yu.* Catalog of large-scale solar wind phenomena for the period 1976-2000 // *Space Research*. V. 47. No. 2. P. 99-113. 2009.
<https://doi.org/10.1134/S0010952509020014>
3. *Zagainova Yu.S., Gromov S.V., Gromova L.I., Feinstein V.G.* Studying the sudden onset of a magnetic storm based on observations with a second time resolution // *Geomagnetism and aeronomy*. V. 64. No. 3. P. 348-362. 2024. <https://doi.org/10.31857/S0016794024030034>
4. *Nishida A.* Geomagnetic diagnosis of the magnetosphere. Translated from English. Moscow: Publishing house "Mir", 306 p. 1980.
5. *Parkhomov V.A.* On the fine structure of the preliminary pulse of the sudden onset of magnetic storms // *Geomagnetism and aeronomy*. V. 25. No. 3. P. 420-424. 1985.
6. *Parkhomov V.A., Borodkova N.L., Yakhnin A.G., Suvorova A.V., Dovbnya B.V., Pashinin A.Yu., Kozelov B.V.* Global pulsed burst of geomagnetic pulsations in the 0.2–5 Hz frequency range as a harbinger of the sudden onset of the St. Patrick's geomagnetic storm on March 17, 2015 // *Space Research*. V. 55. No. 5. P. 323-336. 2017. <https://doi.org/10.7868/S0023420617050016>
7. *Araki T.* Global structure of geomagnetic sudden commencements // *Planet. Space Sci.* V. 25. № 4. P. 373–384. 1977. [https://doi.org/10.1016/0032-0633\(77\)90053-8](https://doi.org/10.1016/0032-0633(77)90053-8)
8. *Araki T.* A physical model of the geomagnetic sudden commencement / *Solar Wind Sources of Magnetospheric Ultra-Low-Frequency Waves*. Eds. M.J. Engebretson, K. Takahashi, M. Scholer. *Geophys. Monograph*. V. 81. Washington, D.C.: AGU. P. 183–200. 1994.
<https://doi.org/10.1029/GM081p0183>
9. *Araki T., Shinbori A.* Relationship between solar wind dynamic pressure and amplitude of geomagnetic sudden commencement (SC) // *Earth Planets Space*. V. 68. ID 90. 2016.
<https://doi.org/10.1186/s40623-016-0444-y>
10. *Bocchialini K., Grison B., Menvielle M. et al.* Statistical analysis of solar events associated with Storm Sudden Commencements over one year of solar maximum during cycle 23: Propagation from the Sun to the Earth and effects // *Solar Phys.* V. 293. N 5. ID 75. 2018.
<https://doi.org/10.1007/s11207-018-1278-5>

11. *Brueckner G.E., Howard R.A., Koomen M.J. et al.* The large angle spectroscopic coronagraph (LASCO) // *Solar Phys.* V. 162. № 1–2. P. 357–402. 1995. <https://doi.org/10.1007/BF00733434>
12. *Curto J.J., Araki T., Alberca L.F.* Evolution of the concept of Sudden Storm Commencements and their operative identification // *Earth Planets Space.* V. 59. P. i–xii. 2007. <https://doi.org/10.1186/BF03352059>
13. *Domingo V., Fleck B., Poland A.I.* The SOHO mission: An overview // *Solar Phys.* V. 162. № 1–2. P. 1–37. 1995. <https://doi.org/10.1007/BF00733425>
14. *Fathy A., Kim K.-H., Park J.-S., Jin H., Kletzing C., Wygant J.R., Ghamry E.* Characteristics of Sudden Commencements observed by Van Allen Probes in the inner magnetosphere // *J. Geophys. Res. – Space.* V. 123. N 2. P. 1295–1304. 2018. <https://doi.org/10.1002/2017JA024770>
15. *Hundhausen A.J.* Coronal expansion and solar wind. Berlin, Heidelberg: Springer-Verlag, 238 p. 1972. <https://doi.org/10.1007/978-3-642-65414-5>
16. *Kikuchi T., Araki T.* Transient response of uniform ionosphere and preliminary reverse impulse of geomagnetic storm sudden commencement // *J. Atmos. Sol.-Terr. Phy.* V. 41. № 9. P. 917–925. 1979. [https://doi.org/10.1016/0021-9169\(79\)90093-X](https://doi.org/10.1016/0021-9169(79)90093-X)
17. *Mayaud P.* Analysis of storm sudden commencements for the years 1868–1967 // *J. Geophys. Res.* V. 80. № 1. P. 111–122. 1975. <https://doi.org/10.1029/JA080i001p00111>
18. *Nishimura Y., Kikuchi T., Ebihara Y., Yoshikawa A., Imajo S., Li W., Utada H.* Evolution of the current system during solar wind pressure pulses based on aurora and magnetometer observations // *Earth Planets Space.* V. 68. ID 144. 2016. <https://doi.org/10.1186/s40623-016-0517-y>
19. *Pezzopane M., Del Corpo A., Piersanti M., Cesaroni C., Pignatelli A., Di Matteo S., Spogli L., Vellante M., Heilig B.* On some features characterizing the plasmasphere–magnetosphere–ionosphere system during the geomagnetic storm of 27 May 2017 // *Earth Planets Space.* V. 71. ID 77. 2019. <https://doi.org/10.1186/s40623-019-1056-0>
20. *Singh Y.P., Badruddin B., Agarwal S.* Occurrence of sudden storm commencement in interplanetary space // *Adv. Space Res.* V. 74. № 10. P. 5252–5262. 2024. <https://doi.org/10.1016/j.asr.2024.07.065>
21. *Smith A.W., Forsyth C., Rae J., Rodger G.J., Freeman M.P.* The impact of Sudden Commencements on ground magnetic field variability: Immediate and delayed consequences // *Space Weather.* V. 19. № 7. ID e2021SW002764. 2021. <https://doi.org/10.1029/2021SW002764>
22. *Sun T.R., Wang C., Zhang J.J., Pilipenko V.A., Wang Y., Wang J.Y.* The chain response of the magnetospheric and ground magnetic field to interplanetary shocks // *J. Geophys. Res. – Space.* V. 120. № 1. P. 157–165. 2015. <https://doi.org/10.1002/2014JA020754>

23. Veretenenko S., Ogurtsov M., Obridko V. Long-term variability in occurrence frequencies of magnetic storms with sudden and gradual commencements // J. Atmos. Sol.-Terr. Phys. V. 205. ID 105295. 2020. <https://doi.org/10.1016/j.jastp.2020.105295>
24. Zhou Y.-L., Lühr H. Initial response of nightside auroral currents to a Sudden Commencement: Observations of electrojet and substorm onset // J. Geophys. Res. – Space. V. 127. № 4. ID e2021JA030050. 2022. <https://doi.org/10.1029/2021JA030050>

FIGURE CAPTIONS

Fig. 1. Comparison of the H-component of the geomagnetic field from data with minute and second temporal resolution for the analyzed SC events from March 17, 2013 (panels on the left) and March 17, 2015 (panels on the right) using data from the low-latitude magnetic observatory HON (*a*, *b*), the mid-latitude observatory CLF (*c*), and the low-latitude magnetic observatories DLT (*d*), TAM (*e*), and LRM (*f*).

Fig. 2. Comparison of the variations of the *H-component* of the magnetic field with 1-second time resolution from the universal time UT from data of different stations, for the SC events on March 17, 2013 (*a*) and March 17, 2015 (*b*), where the dashed circle highlights the time range within which a sharp increase of the *H-component* of the field - MI was observed.

Fig. 3. Variations of the meplanetary magnetic field and solar wind parameters: field modulus $B||$ and Bz (GSE) component: velocity (Speed) V , proton density Np , proton temperature T , and the *SYM/H* Earth storm activity index on March 17, 2015. The arrows show the moments when SC caused by the arrival of the interplanetary shock wave KWM to the Earth and the leading edge of the magnetic cloud were observed.

Fig. 4. Appearance moments of SC (*a*, *c*) and MI (*b*, *d*) as functions of geographic coordinates (latitude φ and longitude relative to the "noon line" λ) of the magnetic observatories and world time UT for the event on March 17, 2015. Regression lines are shown in each plot.

Fig. 5. Same as in Fig. 3, but for the event of March 17, 2013.

Fig. 6. Same as Fig. 4, but for the event of March 17, 2013.

Fig. 7. Illustrations of the orientation of the normal to the MUV in the XZ (a, c, e) and XY (b, d, f) planes in the GSE coordinate system. We neglected the difference of the latitude $\langle\theta\rangle$ and longitude $\langle\varphi\rangle$ of the normal to the MUV front from their absolute values in three-dimensional space.

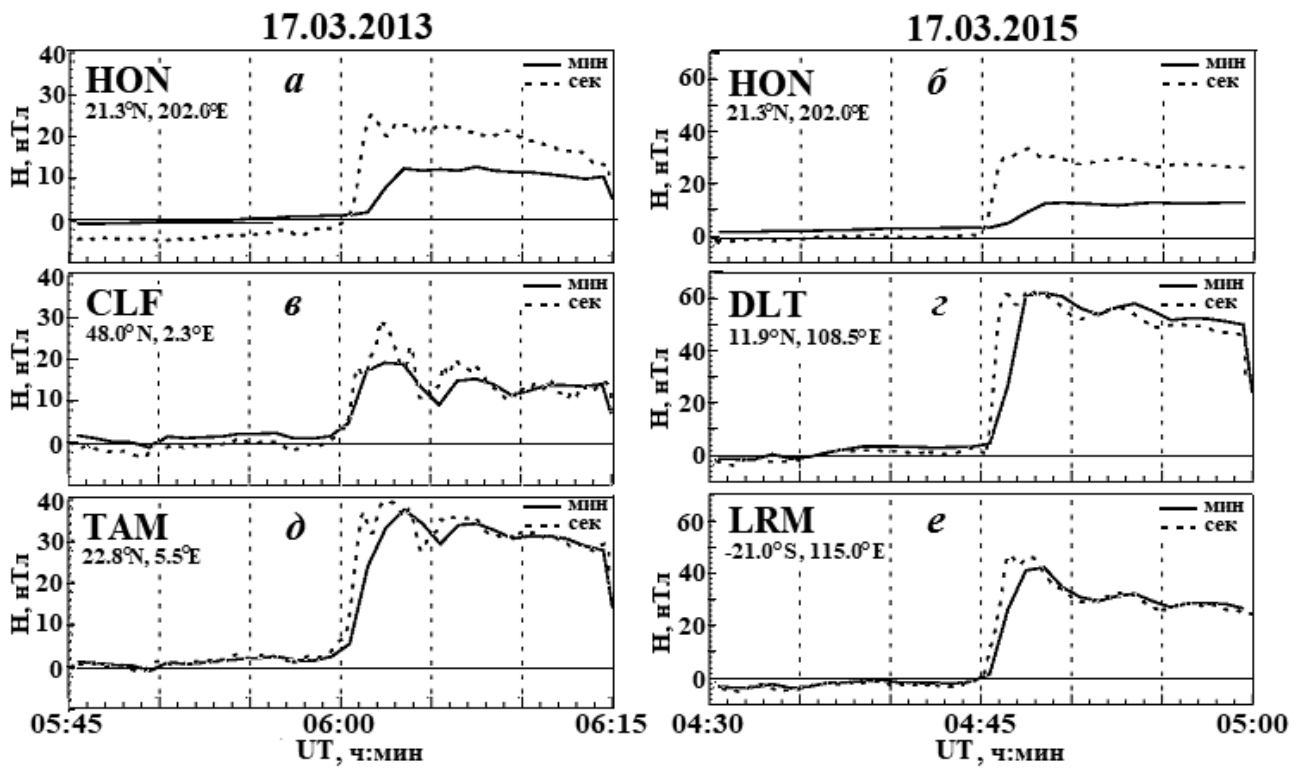


Fig. 1.

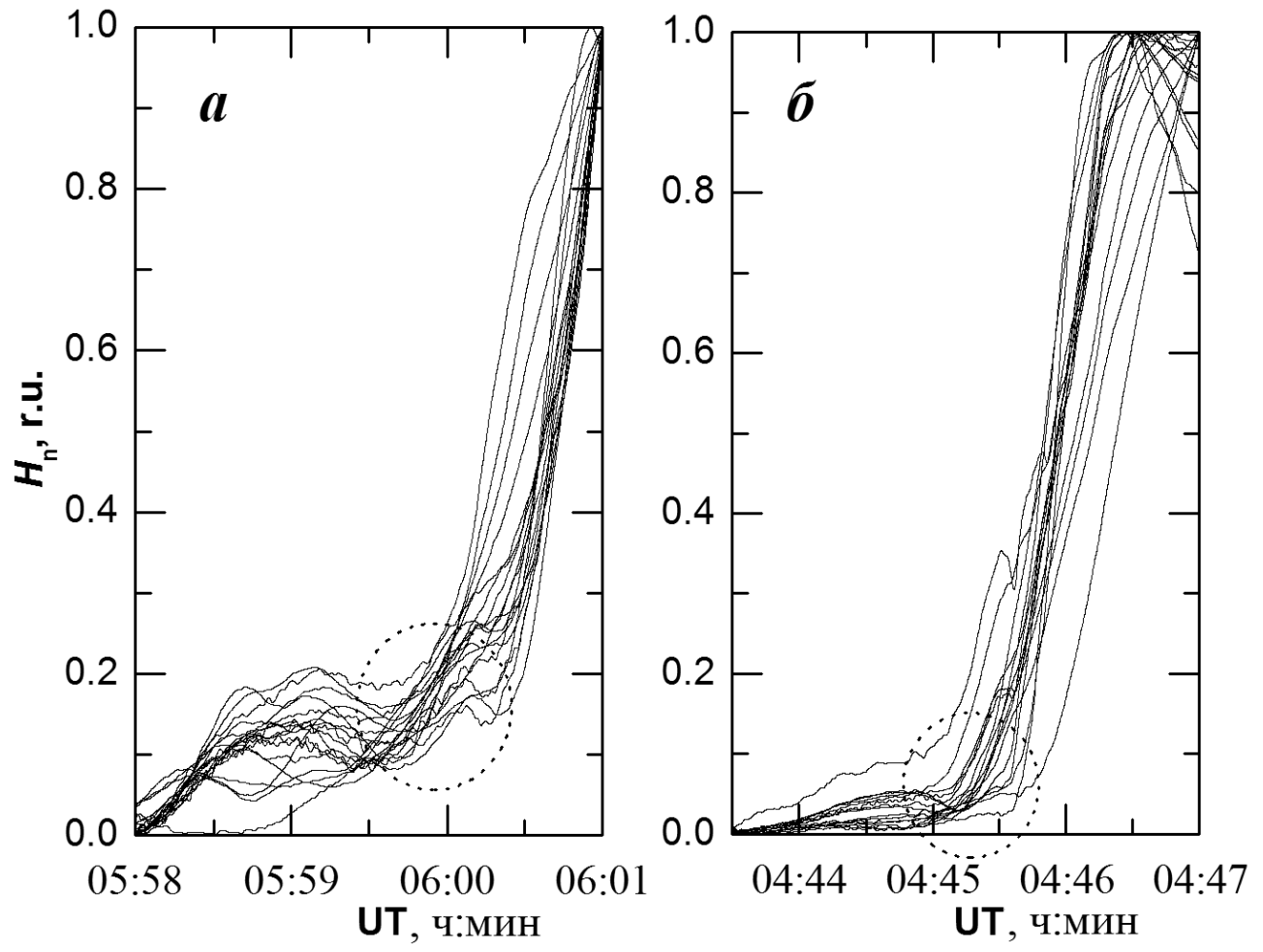


Fig. 2.

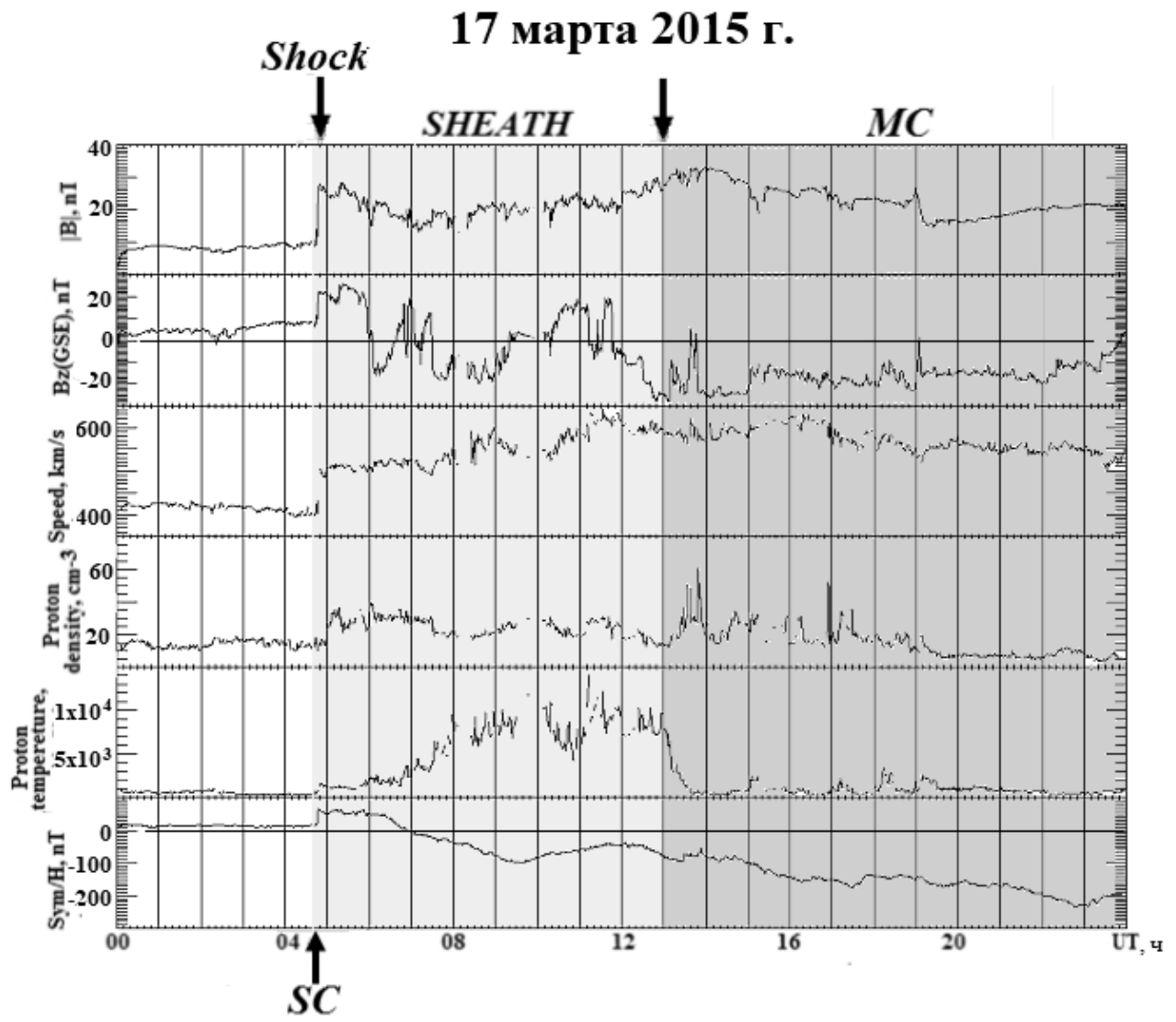


Fig. 3.

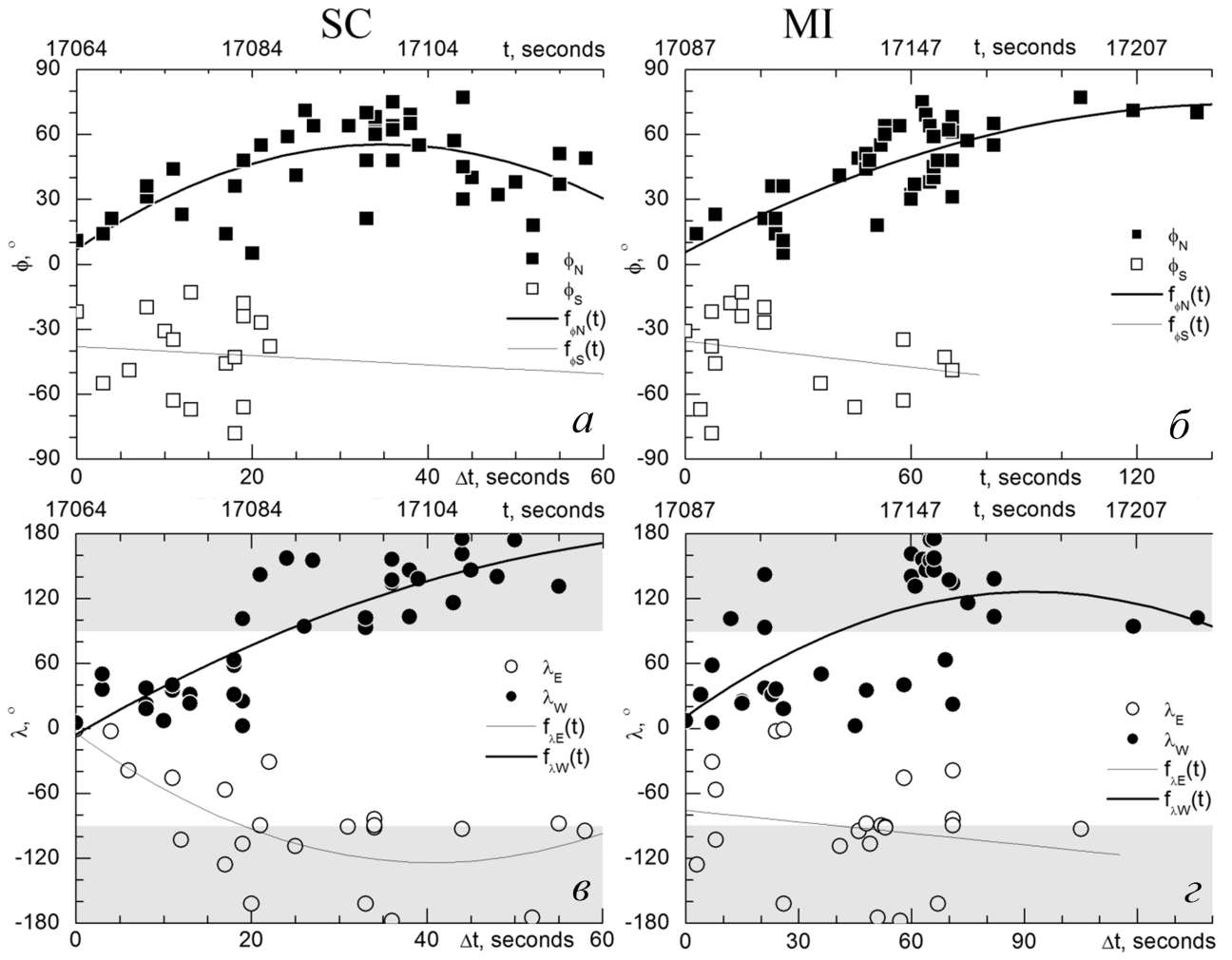


Fig. 4.

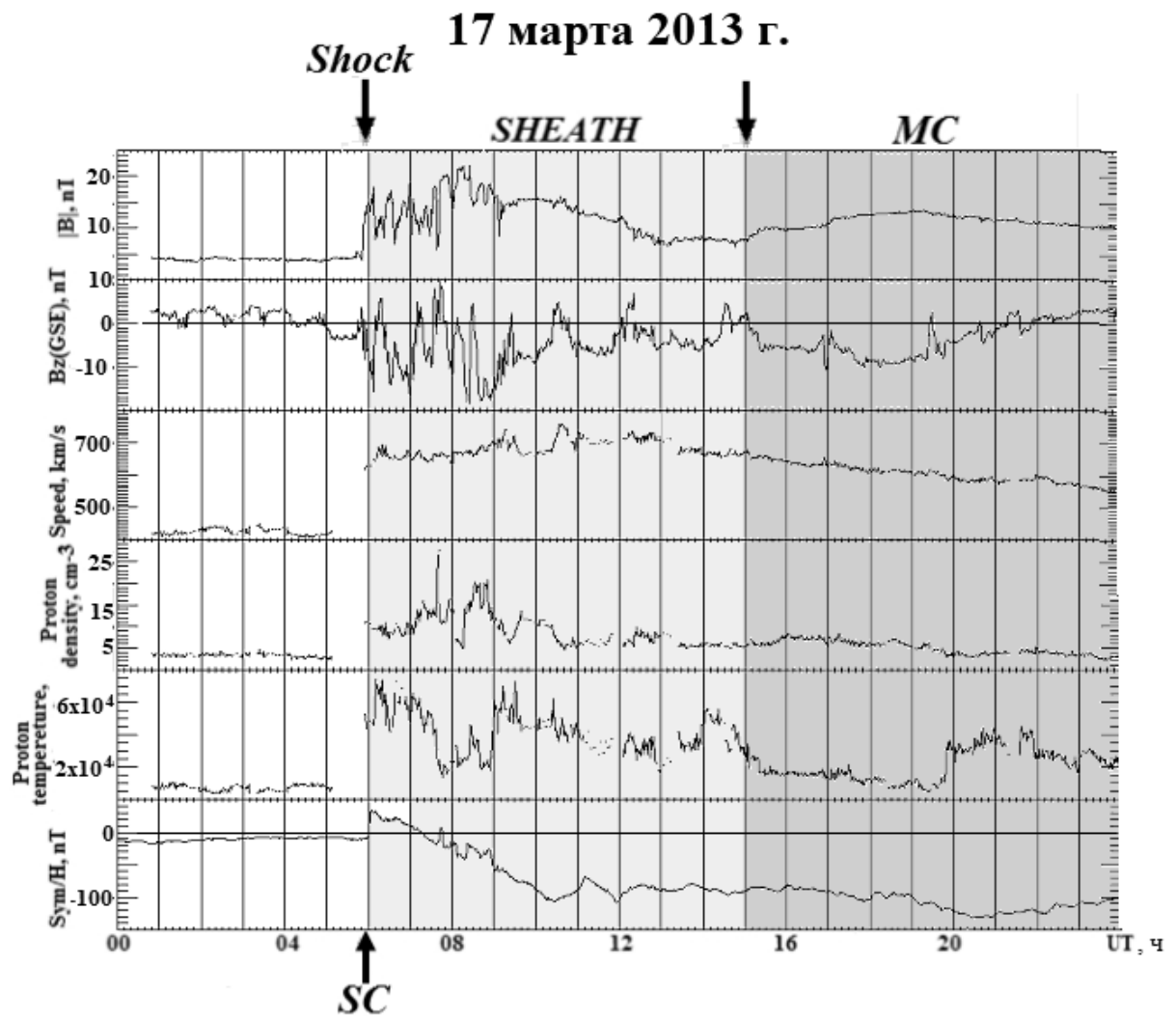


Fig. 5.

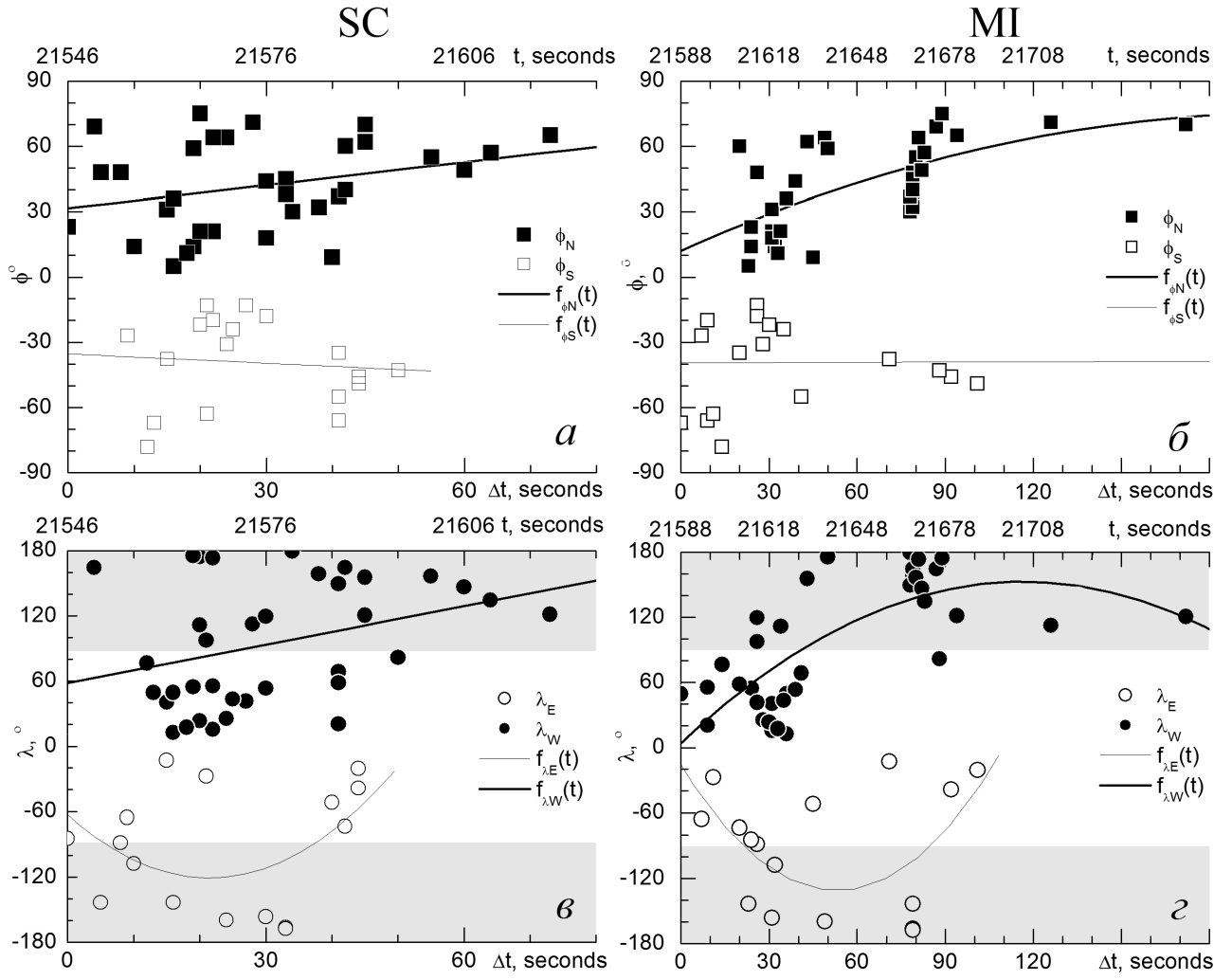


Fig. 6.

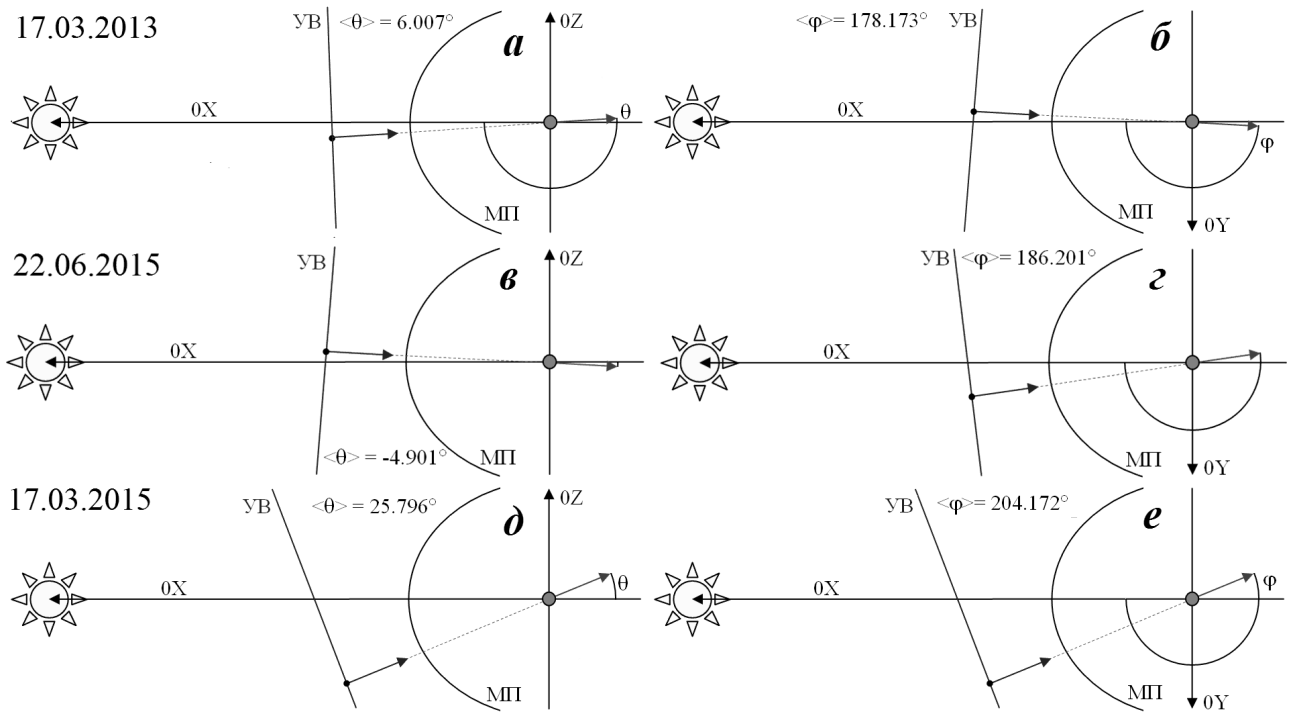


Fig. 7.